

## Microcanonical Monte Carlo simulations for the two-dimensional XY model

This article has been downloaded from IOPscience. Please scroll down to see the full text article.

1992 J. Phys.: Condens. Matter 4 5411

(<http://iopscience.iop.org/0953-8984/4/24/011>)

View [the table of contents for this issue](#), or go to the [journal homepage](#) for more

Download details:

IP Address: 171.66.16.159

The article was downloaded on 12/05/2010 at 12:08

Please note that [terms and conditions apply](#).

## Microcanonical Monte Carlo simulations for the two-dimensional $XY$ model

Smita Ota†, S B Ota‡ and M Föhnle†

† Institut für Physik, Max-Planck-Institut für Metallforschung, Heisenbergstrasse 1, D-7000 Stuttgart 80, Federal Republic of Germany

‡ Max-Planck-Institut für Festkörperforschung, Heisenbergstrasse 1, D-7000 Stuttgart 80, Federal Republic of Germany

Received 28 October 1991, in final form 6 December 1991

**Abstract.** We have carried out microcanonical Monte Carlo (MC) simulations for the two-dimensional (2D) classical  $XY$  model on a square lattice having 900 spins with periodic boundary conditions. The temperature dependence of the energy, specific heat, mean-square magnetization and vortex density show good agreement with the existing canonical MC simulation results. We thus demonstrate ergodicity in the microcanonical MC simulations for the 2D classical  $XY$  model. The maximum of the temperature derivative of the vortex density is found to occur at the temperature corresponding to the maximum of the specific heat.

### 1. Introduction

Monte Carlo (MC) simulations using the Metropolis algorithm [1] have long been a general prescription for computer experiments in statistical mechanics [2]. The algorithm operates in a canonical ensemble, where the temperature ( $T$ ) is the input parameter and the thermodynamic quantities are obtained from the simulation. The method is stochastic in principle. On the other hand, in the case of the microcanonical MC simulation proposed by Creutz [3], the total energy is the input parameter and the temperature is obtained from the simulation. This might have an advantage in some cases [4], because it is expected that the physical quantities depend in a smoother way on the internal energy than on the temperature. An extra degree of freedom called ‘the demon’ (after Maxwell’s demon) travels in the system, transferring energy as it changes the microstate. The method is deterministic in principle and the system complexity is expected to give rise to the ergodicity. To avoid trapping in metastable states some amount of randomness is introduced in the simulation [4]. However, rigorous proof of ergodicity in the deterministic microcanonical MC simulation is lacking [4]. The question of ergodicity has been approached pragmatically in the case of the discrete Ising model [4] by comparing the results of the microcanonical MC simulations with the exact results. There is, however, no literature to our knowledge on microcanonical MC simulations for spin systems with continuous symmetry (the two dimensional (2D) classical  $XY$  model, for example [5]). The absence of long-range order [6], the presence of topological defects called vortices, and the Kosterlitz–Thouless transition [7, 8], are some of the notable properties of

this model. Several canonical MC simulations [9–15] have been performed to study its equilibrium properties. There are also canonical MC simulations based on improved techniques, for instance on an over-relaxed algorithm [16] or on the collective MC updating [17]. However, the simulations in microcanonical ensemble have been performed using the molecular dynamics (MD) algorithm [18]. Here we present the results of microcanonical MC simulations for the 2D classical  $XY$  model and demonstrate ergodicity by comparing with the corresponding canonical MC and microcanonical MD simulations. However, we do not plan to carry out a comparison of the computational efficiencies of the various techniques.

The paper is organized as follows. In section 2, we describe the calculational procedure for the microcanonical MC simulation. The temperature dependence of the energy, specific heat, mean-square magnetization and vortex density are presented in section 3. The conclusions are given in section 4.

## 2. Calculational procedure

The Hamiltonian of the 2D  $XY$  model, with the spins constrained to lie in the plane, is given by

$$H = -J \sum_{\langle i, j \rangle} \cos(\theta_i - \theta_j) \quad (1)$$

where  $J > 0$  is the coupling constant and  $\theta_i$  is the angle made by the spin at site  $i$  with respect to a fixed axis in the plane. The sum  $\langle i, j \rangle$  is over the nearest neighbours. (This is also known as the 2D planar-spin model.) For our simulation, we consider a 2D square lattice having 900 spins with periodic boundary conditions. For simplicity and faster computational speed, the continuous  $\theta$  is discretized. We used 300 discrete states;  $\theta_i = 2\pi n/300$ , where  $n = 1, 2, 3, \dots, 300$ . In this context, we note from the existing canonical MC simulations that even 12 states are sufficient to represent the continuous model near the Kosterlitz–Thouless transition [10].

We performed the microcanonical MC simulations as follows. When the demon with energy  $E_D$  reaches site  $i$ , a random integer number is generated from a uniform distribution in the range  $[-150, 150]$  corresponding to a change in  $\theta_i$  in the range  $[-\pi, \pi]$ . Although the selection of the change in  $\theta_i$  is random, the decision whether the change is accepted or not is deterministic, in contrast to the canonical MC spin updating procedure [1]. The change is accepted if the system lowers (or does not change) the energy which is given to the demon or if the system needs energy from the demon and the demon has sufficient energy to allow the change. Otherwise, the old state is retained and the demon moves to the next site. In this manner, the demon is allowed to visit all the sites of the lattice sequentially and this constitutes one Monte Carlo step per spin (MCSS) of the simulation. This criterion for the choice of the change in  $\theta_i$  satisfies a restricted form of detailed balance [3] in order to approach a uniform distribution of microstates. Moreover, the introduction of randomness in the change of  $\theta_i$  also helps in achieving ergodicity. In equilibrium, the demon energy obeys the Boltzmann distribution function (figure 1). The demon works like a thermometer for the heat bath represented by the spin system. For the case where  $E_D$  takes continuous positive values, the temperature is directly related to the average demon energy  $\langle E_D \rangle$  [3]:

$$\langle E_D \rangle = k_B T \quad (2)$$

where  $k_B$  is the Boltzmann constant. (Hereafter we replace  $k_B T/J$  by  $T$  and  $E/J$  by  $E$  for

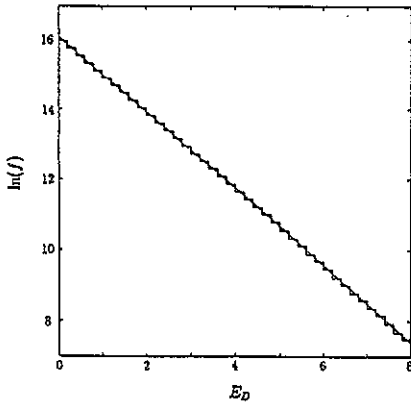


**Figure 1.** The distribution of demon energies over  $5 \times 10^4$  MCSS after  $7 \times 10^4$  MCSS used for the equilibration. The initial configuration was with all the spins parallel to each other. The ordinate represents the natural logarithm of the number of times out of  $45 \times 10^6$  steps that the demon is in the corresponding energy bin of width 0.2. The straight line represents the Boltzmann distribution for the corresponding temperature of 0.919.

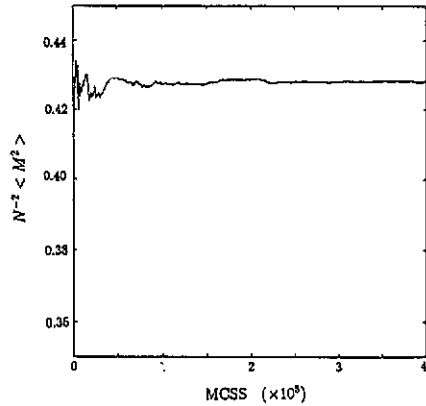


**Figure 2.**  $N^{-2}\langle M^2 \rangle$  as a function of MCSS. The initial configuration was with all spins parallel to each other. Each point on the curve represents the average over all the configurations starting from the first MCSS to a given MCSS. The corresponding temperature is 0.919.

simplicity.) Although the spin states are discretized in our case,  $E_D$  can take continuous value. Therefore, we estimate the temperature from the average demon energy (2). We used only the final  $E_D$  after each MCSS to calculate the corresponding temperature for the Boltzmann distribution (represented by the straight line in figure 1). The equilibrium of the mean-square magnetization per spin ( $N^{-2}\langle M^2 \rangle$ ) with this algorithm is shown in figure 2. The mean-square magnetization per spin is defined as,

$$N^{-2}\langle M^2 \rangle = N^{-2} \left\langle \left( \sum_{i=1}^N \cos \theta_i \right)^2 + \left( \sum_{i=1}^N \sin \theta_i \right)^2 \right\rangle \quad (3)$$

where  $N$  is the total number of spins. We used the final  $M^2$  after each MCSS for the average in  $\langle M^2 \rangle$ .

The cooling cycle of the simulation proceeded as follows. Initially all the spins were aligned parallel to each other (i.e.  $\theta_i = 2\pi$ ). The demon was given a fixed amount of energy which, when added to the initial system energy, corresponds to the energy at the highest desired temperature. Typically we used  $3 \times 10^4$  MCSS ( $2.5 \times 10^4$  MCSS) for equilibration and  $7 \times 10^4$  MCSS ( $5 \times 10^4$  MCSS) for averaging near (away from) the Kosterlitz–Thouless transition. The physical quantities calculated after each MCSS were used for the averaging. The accuracy of the mean value of the physical quantities was estimated by performing block averages consisting of  $5 \times 10^3$  MCSS each and then finding the standard deviation of the block averages. The total energy ( $E_T$ ), equal to the demon energy ( $E_D$ ) plus the energy of the spin system ( $E_S$ ), remains constant for each simulation run. We obtained  $\langle E_S \rangle$  by subtracting  $\langle E_D \rangle$  from the total energy  $E_T$ . The temperature of the spin system was obtained from the average  $E_D$  using the demon energy after each MCSS. The final spin configuration and  $E_D$  were retained after the simulation run. The next lower temperature was obtained by subtracting a finite amount of energy from the

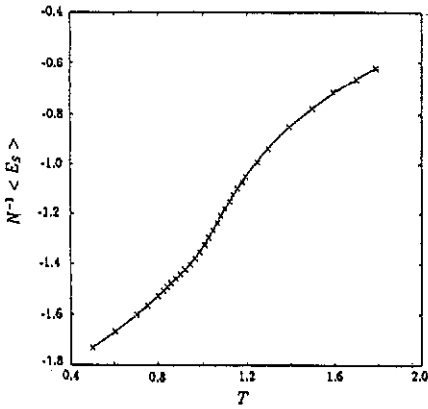


Figure 3. Average system energy per spin as a function of temperature. The solid line is the least-squares cubic spline fit to the data points.

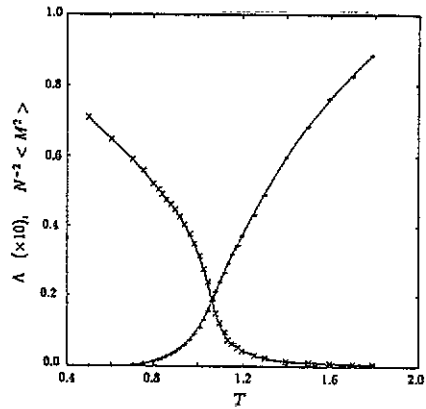


Figure 4.  $\Lambda$  (+) and  $N^{-2}\langle M^2 \rangle$  ( $\times$ ) as functions of temperature. The solid lines are the least-squares cubic spline fits to the data points.

demon and proceeding through the simulation. This procedure is repeated until the lowest desired temperature is reached. The system was then heated stepwise through the same total energies as those of the cooling cycle. During the heating cycle, energy was added to the spin system through the demon. The results of the cooling run and the heating run did not differ by more than 1%. The physical quantities presented in the following section are the average of the cooling and the heating run at each  $E_T$ .

### 3. Results

The temperature dependence of the average system energy per spin  $N^{-1}\langle E_S \rangle$  is displayed in figure 3. The standard deviation of the estimated temperature is less than about 0.5%. We also calculated the temperature dependence of  $N^{-1}\langle M^2 \rangle$  and the vortex density ( $\Lambda$ ).  $\langle M^2 \rangle$  is related to the susceptibility ( $\chi$ ) as follows:

$$\chi = (NT)^{-1}(\langle M^2 \rangle - \langle M \rangle^2). \quad (4)$$

The spontaneous magnetization of the 2D classical XY model should vanish at all finite temperatures [10, 11] and therefore  $\chi$  is estimated as being equal to  $(NT)^{-2}\langle M^2 \rangle$ . The reasoning behind this approach [10] is that  $\langle M^2 \rangle$  is rather stable against the number of MCSS, whereas  $\langle M \rangle$  is not necessarily small at intermediate steps, and it goes to zero gradually. Figure 4 displays the temperature dependence of  $N^{-2}\langle M^2 \rangle$ . The standard deviation of the calculated  $N^{-2}\langle M^2 \rangle$  is less than 4%.

The presence of vortices in the 2D classical XY model, which was postulated theoretically [7, 8], has been examined in several computer simulations [9–11, 14, 17, 18]. The Kosterlitz–Thouless theory defines the vorticity  $q$  of a given region as follows [8]:

$$q = \frac{1}{2\pi} \oint d\theta(r). \quad (5)$$

Here the integral is taken round the boundary of that region and  $\theta(r)$  is the angle which a spin situated at  $r$  makes with the fixed axis. We used a discrete version of the above

definition of  $q$  to calculate the vorticity in each elementary square plaquette consisting of four spins at the corners. The total number of positive vortices was found to be equal to the total number of negative vortices, which is a consequence of the periodic boundary conditions [11]. We define the vortex density  $\Lambda$  as the total number of positive (or negative) vortices divided by the number of spins. Figure 4 shows the temperature dependence of the vortex density. The standard deviation of the calculated vortex density is typically less than 0.5%.

In table 1, we compare  $N^{-1}\langle E_S \rangle$ ,  $N^{-2}\langle M^2 \rangle$  and  $\Lambda$  obtained from the present microcanonical MC simulations with that of the existing canonical MC [10, 11, 15, 18] and microcanonical MD [18] simulations. The values corresponding to the microcanonical MC simulations for the fixed temperatures are obtained from the least-squares cubic spline fits of the data (figures 3 and 4). It is seen from table 1 that the present microcanonical MC simulation results agree with that of the existing canonical MC and microcanonical MD simulations. In this context, we note that canonical and microcanonical ensembles give identical results only in the thermodynamic limit. However, the difference between these two ensembles for a 900 spin system is numerically small, as has been noted by Kogut and Polonyi (reference [18] in table 1).

Next we examine the specific heat ( $C$ ). Several canonical MC simulations [11–13] show that the maximum in the temperature dependence of the specific heat occurs at a temperature which is about 15% higher than the Kosterlitz–Thouless transition temperature. We have calculated the specific heat from the relation  $C = N^{-1}(\partial\langle E_S \rangle/\partial T)$ . The temperature dependence of the specific heat is shown in figure 5 along with the temperature dependence of  $\partial\Lambda/\partial T$ . The temperature derivatives were obtained from the least-squares cubic spline fits of the data. We obtain the specific heat peak at 1.09 with a peak height of 1.56. This is comparable to the reported values of the peak position (peak height) of 1.02 (1.55) for 900 spins [11], 1.07 for 1024 spins (McMillan as quoted in [11]), 1.06 (1.45) for 3600 spins [12] and 1.07 (1.44) for 1600 spins [13]. We also found that the maximum in  $\partial\Lambda/\partial T$  occurs at 1.10 which is equal to the temperature at which the specific heat peak occurs, within the uncertainties of the data. This observation can be naively understood as follows. Formation of a vortex costs energy and therefore the temperature rate of change of the vortex density is directly related to the temperature rate of change of  $\langle E_S \rangle$ . Hence, one expects that the maxima of  $C(T)$  and  $\partial\Lambda/\partial T$  should occur at the same temperature. The Kosterlitz–Thouless transition, which is associated with the unbinding of the vortex–antivortex pair, however, occurs at a lower temperature of about 0.9 [11–13, 15, 16].

#### 4. Conclusions

We have presented the microcanonical MC simulations for the 2D classical  $XY$  model based on the method proposed by Creutz [3]. We obtain good agreement of the temperature dependences of  $N^{-1}\langle E_S \rangle$ ,  $N^{-2}\langle M^2 \rangle$ ,  $\Lambda$  and  $C$  with that obtained from the existing canonical MC and microcanonical MD simulations. We have thus demonstrated ergodicity in the microcanonical MC simulations for the 2D classical  $XY$  model in an equilibrium situation. We also find that the maximum of the temperature derivative of the vortex density occurs at the temperature corresponding to the maximum of the specific heat.

Here, we have not compared the computational efficiencies of the various techniques. The critical slowing down is one of the main factors which affects the computational efficiency. In this respect, there are improved canonical MC simulation

Table 1. Comparison with the canonical MC and microcanonical MD simulations (all quantities are per spin).

T	$N^{-1}\langle E_S \rangle$				$N^{-2}\langle M^2 \rangle$				$\Lambda$	
	Ref. [11]	Ref. [18]	Ref. [18] (MD)	Present study	Ref. [10]	Ref. [15]	Present study	Ref. [18]	Ref. [18] (MD)	Present study
0.50	-1.730	—	—	-1.730	0.7054	—	0.7107	—	—	0.0000
0.90	-1.438	—	—	-1.441	0.4427	0.3522	0.4426	—	—	0.0043
1.00	-1.3310	—	-1.3153	-1.329	0.2971	0.2078	0.3251	0.0113	0.0116	0.0108
1.10	-1.1864	-1.3257	—	-1.182	0.1148	0.0898	0.1171	—	—	0.0238
1.20	-1.055	—	-1.0376	-1.041	0.0512	0.0400	0.0453	0.0372	0.0385	0.0378
1.30	-0.952	-1.0490	—	-0.935	—	0.0208	0.0232	—	—	0.0498
1.60	-0.731	—	—	-0.718	—	—	0.0088	—	—	0.0764

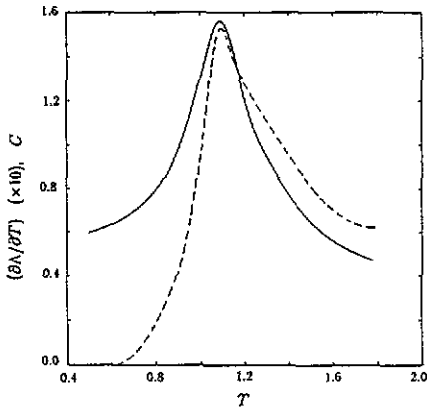


**Figure 5.**  $C$  (solid line) and  $\partial\Lambda/\partial T$  (dashed line) as functions of temperature. Specific heat is given by  $N^{-1}(\partial\langle E_S \rangle/\partial T)$ . Both  $\partial\langle E_S \rangle/\partial T$  and  $\partial\Lambda/\partial T$  were obtained from the least-squares cubic spline fitted curves in figures 3 and 4. The maxima of  $C$  and  $\partial\Lambda/\partial T$  occur at temperatures 1.09 and 1.10, respectively.

techniques [16, 17] to reduce the effect of the critical slowing down. One important aspect of the present microcanonical MC simulation is that the number of computational operations does not increase by increasing the number of spin states, unlike the conventional canonical MC simulation [10]. This feature allows one to increase the number of spin states at will, without practically slowing down the speed of simulation. It is straightforward to extend this algorithm to any other spin model with continuous symmetry.

### Acknowledgments

We thank E Gmelin for helpful discussions and G Zumbach for critical reading of this manuscript.

### References

- [1] Metropolis N, Rosenbluth A, Rosenbluth M, Teller A and Teller E 1953 *J. Chem. Phys.* **21** 1087
- [2] Mouritsen O G 1984 *Computer Studies of Phase Transitions and Critical Phenomena (Springer Series in Computational Physics)* (Berlin: Springer)
- Binder K and Stauffer D 1984 *Applications of the Monte Carlo Method in Statistical Physics (Topics in Current Physics 36)* ed K Binder (Berlin: Springer) p 1
- [3] Creutz M 1983 *Phys. Rev. Lett.* **50** 1411
- [4] Bhanot G, Creutz M and Neuberger H 1984 *Nucl. Phys. B* **235** 417
- [5] Ma S K 1985 *Statistical Mechanics* (Singapore: World Scientific) ch 29, pp 495–8
- [6] Mermin N D and Wagner H 1966 *Phys. Rev. Lett.* **17** 1133
- [7] Berezinskii V L 1970 *Sov. Phys.-JETP* **32** 493
- [8] Kosterlitz J M and Thouless D J 1972 *J. Phys. C: Solid State Phys.* **5** L124; 1973 *J. Phys. C: Solid State Phys.* **16** 1181
- Kosterlitz J M 1974 *J. Phys. C: Solid State Phys.* **7** 1046
- [9] Kawabata C and Binder K 1977 *Solid State Commun.* **22** 705
- [10] Miyashita S, Nishimori H, Kuroda A and Suzuki M 1978 *Prog. Theor. Phys.* **60** 1669
- [11] Tobochnik J and Chester G V 1979 *Phys. Rev. B* **20** 3761
- [12] Shugard W J, Weeks J D and Gilmer G H 1980 *Phys. Rev. B* **21** 5309
- [13] Himbergen J E V and Chakravarty S 1981 *Phys. Rev. B* **23** 359
- [14] Betsuyaku H 1981 *Physica A* **106** 311



- [15] Fernández J F, Ferreira M F and Stankiewicz J 1986 *Phys. Rev. B* **34** 292
- [16] Gupta R, Delapp J, Batrouni G G, Fox G C, Baillie C F and Apostolakis J 1988 *Phys. Rev. Lett.* **61** 1996
- [17] Wolff U 1989 *Nucl. Phys. B* **322** 759
- [18] Kogut J and Polonyi J 1986 *Nucl. Phys. B* **265**[FS15] 313